5th International Conference on Experimental Fluid Mechanics – ICEFM 2018 Munich
Munich, Germany, July 2-4, 2018

Incipient particle motion at low particle Reynolds numbers

J. R. Agudo[1,2], S. Dasilva[1], N. Topic[1], A. Wierschem*

[1] Institute of Fluid Mechanics, Friedrich-Alexander-Universität Erlangen-Nürnberg (FAU), Erlangen, Germany

[2] Institute of Fluid Mechanics, FAU Busan Campus, Busan, Republic of Korea

*andreas.wierschem@fau.de

Abstract

We study flow-induced particle motion on regular substrates at low particle Reynolds numbers. The shear flow is created and controlled with a rotational rheometer in the parallel-disk configuration. Particle rotation is detected using marks on the surface of the mobile beads. At the onset of motion, we find that single mobile beads carry out a rolling motion along the substrate, irrespectively of their degree of exposure, angle of repose or deviations from spherical shape.

1 Introduction

Bedload transport and incipient particle motion is encountered in a wide range of industrial and natural processes, ranging from sediment transport in river and oceans to conveying and cleaning of surfaces, see e.g. Burdick et al. (2005), Wierschem et al. (2008), Stevanovic et al. (2014), to name just a few. Due to its broad range of application, flow-induced incipient particle motion has been studied extensively for decades, yet mostly under turbulent conditions (e.g. Yalin and Karahan 1979; Valyrakis et al. 2010). However, during the last decade, also incipient motion in laminar flows, where the wide spectrum of length scales interacting with the bed is avoided (Derksen and Larsen 2011), has been studied intensively, see e.g. Charru et al. (2004), Ouriemi et al. (2007), Seizilles et al. (2014), Hong et al. (2015), Agudo et al. (2017a).

The threshold for the onset of granular motion depends on the type of motion (Ling 1995; Agudo et al. 2017a). The particle motion is typically characterized by rolling, sliding, and bouncing (Charru et al. 2004; Ouriemi et al. 2009). There have been many approaches to study flow induced particle motion at surfaces and in bedload transport (see e.g. Lee et al. 2000; Papanicolau and Knapp 2006; Böhm et al. 2006; Wierschem et al. 2008; Agudo et al. 2017b). Here, we focus on the particle motion close to onset at low particle Reynolds numbers. The substrate consists of a monolayer of regularly arranged fixed beads. Particle rotation is detected using marks on the surface of the beads.

2 Experimental set-up

The experiments were carried out placing a single glass bead with a density of (2.530 ± 0.025) g cm^{-3} and a diameter of (405.9 ± 8.7) µm on a regular substrate made of spheres of same size. The substrate had a size of 15 x 15 mm². It was arranged in quadratic order with a spacing between the spheres of about 14 µm. The regular spacing was obtained by depositing and gluing the glass beads on a stainless steel sieve. The substrate was fixed on a support and placed on the bottom of a circular container with an inner diameter of 176 mm and with 25 mm high sidewalls made from Plexiglas. The container was placed in a rotational rheometer. The mobile bead was placed on top of the substrate center. The substrate was placed off-centered

into the container such that the mobile bead was at a distance of 21 mm from the turning axis of the rheometer. As rotating top plate in our parallel-disk configuration, we used a glass plate of 65 mm diameter.

As liquid, we used a silicon oil with a viscosity of (103.0 ± 3.3) mPas and a density of (0.965 ± 0.005) g/cm^3 at a temperature of (295.16 ± 0.5) K. The laminar shear flow was set up and controlled with the rheometer. The shear flow was characterized by the shear-rate given by $\dot{\gamma} = \Omega r/h$, where Ω, r, h are plate angular velocity, radial distance between mobile particle and turning axis of the rheometer, and the gap width between the top of the substrate and the rotating rheometer plate, respectively. The experiments were carried out at a gap width of 2 mm. We study the particle motion at the critical Shields number for incipient motion. The Shields number, θ, is defined by:

$$\theta = \frac{\nu\dot{\gamma}}{(\rho_S/\rho - 1)ghD_S}, \tag{1}$$

where ν, ρ_S, ρ, g, D_S indicate kinematic viscosity, bead density, fluid density, acceleration of gravity and bead diameter, respectively. The particle Reynolds number, defined by

$$Re_P = \frac{\dot{\gamma}h}{\nu}\left(\frac{D_S}{h}\right)^2 \tag{2}$$

remained below 1 for all experiments.

The particles were illuminated and detected through the rotating disk. To analyze the particle motion, the mobile beads were marked. The locations of the mobile bead and of the markers were tracked in a sequence of images and evaluated with image processing software, see Agudo et al. (2017b) for details: The bead was identified after cropping the images by applying Canny edge detection and circular Hough transform. As a precondition for the mark identification, the marks had to be within the area of the identified bead. They were recognized by appropriate thresholding. For further details on the substrate preparation and on the setup we refer to Agudo and Wierschem (2012), Agudo et al. (2014), and particularly to Agudo et al. (2018).

3 Experiments

First, we studied the rotating incipient motion of a single spherical bead on the substrate. Therefore, we determined the rotation angle of the bead following the marks on the bead and compared their position to that of the bead. Figure 1 depicts the angle of rotation from the initial position to the adjacent equilibrium position as a function of the relative trajectory between two neighboring valleys along the substrate. The experimental results are compared to the angle for a pure rolling motion. The diagram shows that the bead fulfilled a pure rolling motion while traveling along the substrate. This also holds for beads of other materials and on other substrates (Agudo et al. 2014).

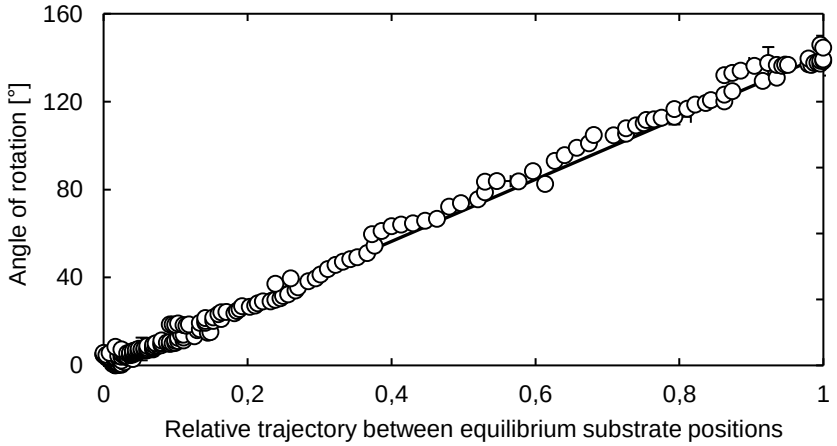

Figure 1: Angle of rotation for a single bead. The line indicates the angle of rotation for a pure rolling motion.

Next, we considered a bead that was completely surrounded by neighboring immobile particles. To this end, we built a cage with tungsten-carbide/cobalt (94:6) beads of same diameter as the glass beads. They have a density of (14.95 ± 0.03) g cm^{-3}. Due to the much higher density they remained immobile in the shear flow that moved the hidden mobile glass bead. The initial motion ended once the bead touched its neighbor in front. The bead left the cage only beyond a Shields number that was almost 8 times larger than the critical one for an exposed bead. We remark that adding further immobile beads did not have any effect on the critical Shields number. Evaluating the motion of the marks on the bead surface showed that rolling was again the mechanism of motion at onset. Figure 2(a) provides an example for the upwinding bead motion. Figure 2(b)-(d) depict snapshots during the climb over the neighbors. The starting position, where the bead was in contact with two neighbors, is shown in Figure 2(b). For this position, the pivot angle is about 85.7°. We remark that the bead reached this position by rolling from its equilibrium position in the valley of the substrate (not shown). In a later stage, when the bead was close to the plateau on top of the neighbors, the bead became more exposed to the flow and deviations from pure rolling motion were observed.

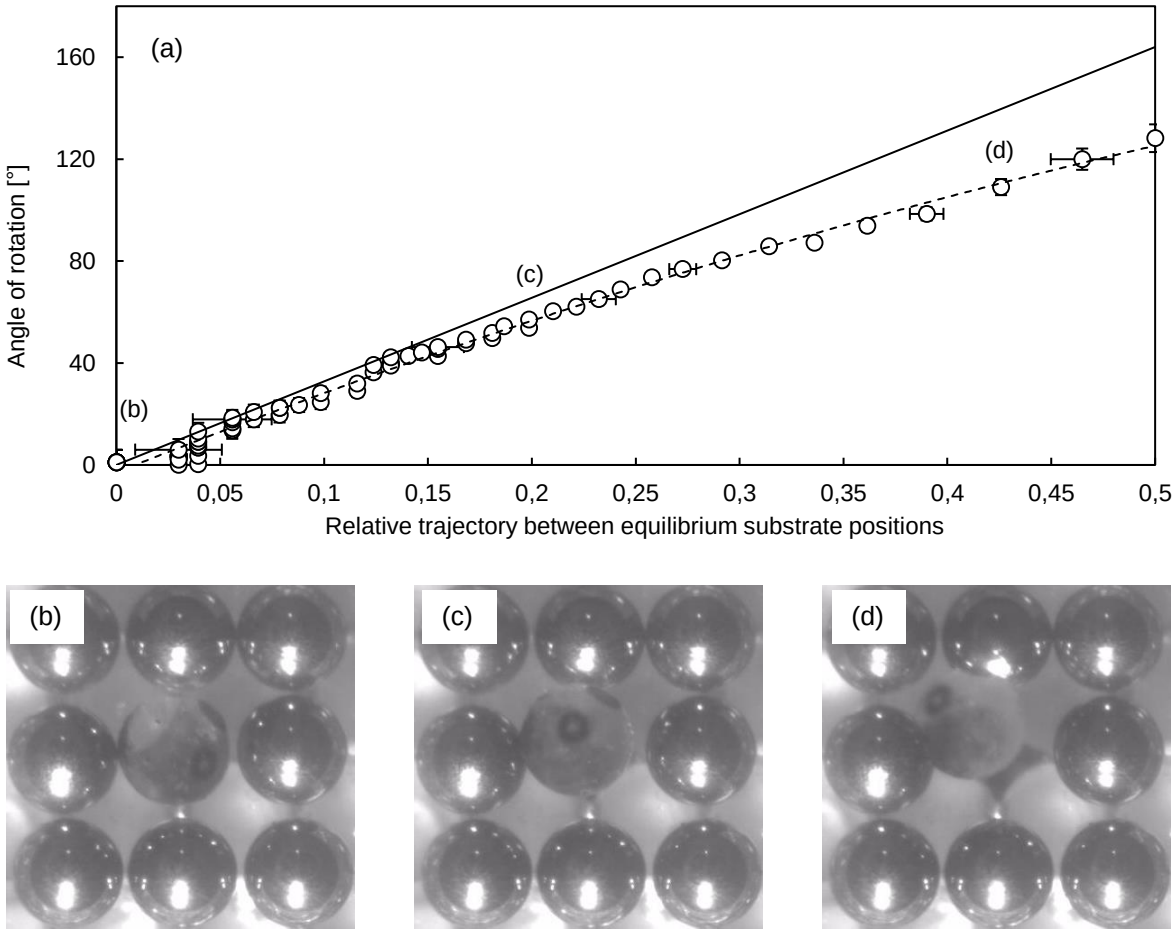

Figure 2: (a) Angle of rotation for an entirely hidden single bead during the climb over the neighbors. The solid line represents the angle of rotation for a pure rolling motion. The dotted line is shown to guide the eye. (b)-(d): Snapshots during dislodgment of the marked bead. The time instances are indicated in the diagram. Flow is from right to left.

To see, whether rolling motion also prevails where deviations from spherical shape are significant, we prepared a dumbbell formed by two beads glued together. As shows Figure 3 even a dumbbell performs a rolling motion.

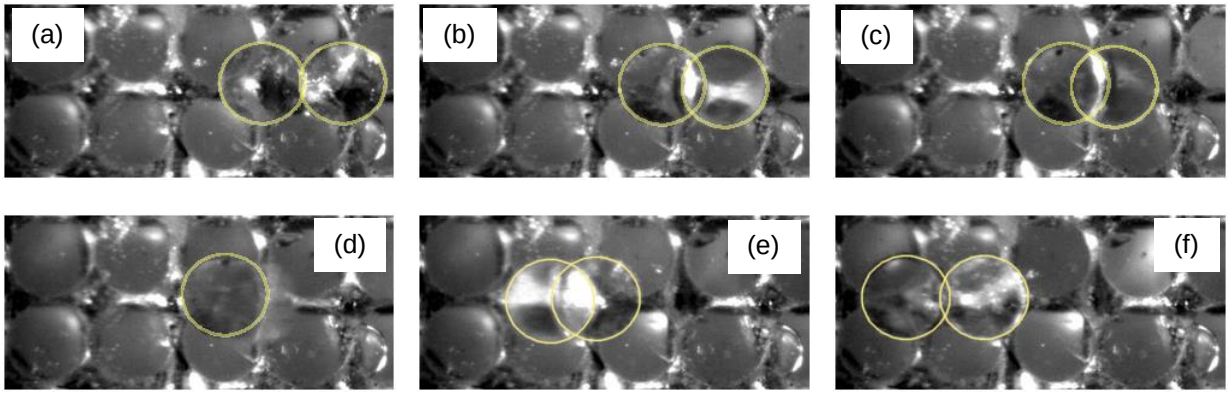

Figure 3: Sequence of pictures showing a top view of two glass beads glued together during the incipient rolling motion. The beads forming the dumbbell are marked to guide the eye. Flow is from right to left.

4 Conclusion

We examined different configurations for flow-induced particle motion on a regular substrate: a single exposed bead and a bead caged by immobile spheres of same size. Deviation from spherical shape were considered with a dumbbell formed by two beads. In all studied cases, we find that the beads rolled during the incipient motion.

Acknowledgements

This study is part of a project supported by Deutsche Forschungsgemeinschaft through WI 2672/4-1 and WI 2672/7-1, which is gratefully acknowledged.

References

Agudo JR, Dasilva S, and Wierschem A (2014) How do neighbors affect incipient particle motion in laminar shear flow? *Physics of Fluids* 26:053303

Agudo JR, Han J, Park J, Kwon S, Loekman S, Luzi G, Lichtenberger C, Delgado A, and Wierschem A (2018) Visually based characterization of the incipient particle motion in regular substrates: From laminar to turbulent conditions. *Journal of Visualized Experiments* 132:e57238

Agudo JR, Illigmann C, Luzi G, Laukart A, Delgado A, Wierschem A (2017a) Shear-induced incipient motion of a single sphere on uniform substrates at low particle Reynolds numbers. *Journal of Fluid Mechanics* 825:284-314

Agudo JR, Luzi G, Han J, Hwang M, Lee J, and Wierschem A (2017b) Detection of granular motion using image processing with particular emphasis on rolling motion. *Review of Scientific Instruments* 88:051805

Agudo JR and Wierschem A (2012) Incipient motion of a single particle on regular substrates in laminar shear flow. *Physics of Fluids* 24:093302

Böhm T, Frey P, Ducottet C, Ancey C, Jodeau M, and Rebaud JL (2006) Two-dimensional motion of a set of particles in a free surface flow with image processing. *Experiments in Fluids* 41:1-11

Burdick G, Berman N, and Beaudoin S (2005) Hydrodynamic particle removal from surfaces. *Thin Solid Films* 488:116-123

Charru F, Mouilleron H, and Eiff O (2004) Erosion and deposition of particles on a bed sheared by a viscous flow. *Journal of Fluid Mechanics* 519:55-80

Derksen J and Larsen R (2011) Drag and lift forces on random assemblies of wall-attached spheres in low-Reynolds-number shear flow. *Journal of Fluid Mechanics* 673:548-573

Hong A, Tao M, and Kudrolli A (2015) Onset of erosion of a granular bed in a channel driven by fluid flow. *Physics of Fluids* 27:013301

Lee HY, Chen YH, You JY, and Lin YT (2000) Investigations of continuous bed load saltating process. *Journal of Hydraulic Engineering* 126:691-700

Ling CH (1995) Criteria for incipient motion of spherical sediment particles. *Journal of Hydraulic Engineering* 121:472-478

Ouriemi M, Aussillous P, Medale M, Peysson Y, and Guazzelli É (2007) Determination of the critical Shields number for particle erosion in laminar flow. *Physics of Fluids* 19:061706

Ouriemi M, Aussillous P, and Guazzelli É (2009) Sediment dynamics. Part 1. Bed-load transport by laminar shearing flows. *Journal of Fluid Mechanics* 636:295-319

Papanicolau AN and Knapp D (2006) A particle tracking technique for bedload motion. *Proceedings of the 7th International Conference on Hydroscience and Engineering*

Seizilles G, Lajeunesse E, Devauchelle O, and Bak M (2014) Cross-stream diffusion in bedload transport. *Physics of Fluids* 26:013302

Stevanovic VD, Stanojevic MM, Jovovic A, Radic DB, Petrovic MM, Karlicic NV (2014) Analysis of transient ash pneumatic conveying over long distance and prediction of transport capacity. *Powder Technology* 254:281-290

Valyrakis M, Diplas P, Dancey CL, Greer K, and Celik AO (2010) Role of instantaneous force magnitude and duration on particle entrainment. *Journal of Geophysical Research: Earth Surface* 115:F02006

Wierschem A, Groh C, Rehberg I, Aksel N, and Kruelle CA (2008) Ripple formation in weakly turbulent flow. *European Physics Journal E* 25:213-221

Yalin MS and Karahan E (1979) Inception of sediment transport. *Journal of Hydraulic Engineering* 105:1433-1443